Phase velocity statistics in random textured polycrystals

Shahram Khazaie, Ningyue Sheng, Mathilde Chevreuil, Sylvain Freour

CSMA 2024
16ème Colloque National en Calcul des Structures
13-17 Mai 2024, Presqu'île de Giens (Var)

Phase velocity statistics in random textured polycrystals

S. Khazaie[1], N. Sheng[1], M. Chevreuil[1], S. Fréour[1]

[1] *Nantes Université, Ecole Centrale Nantes, CNRS, GeM, UMR 6183, F-44000 Nantes, France*
{shahram.khazaie,ningyue.sheng,mathilde.chevreuil,sylvain.freour}@univ-nantes.fr

Abstract — In real finite-sized polycrystals, the background elastic properties are no longer deterministic. Consequently, the corresponding phase velocities and attenuation coefficients also become random. Recently, we showed that second-order statistics of polycrystals' effective elastic modulus tensor and the phase velocities reveal microstructural information such as the mean and standard deviation of grain size. In this paper, we extend the results to the case of textured polycrystals. The analytical framework is valid for cubic equiaxed grains with arbitrary grain size distribution and crystallographic texture level. The variabilities the phase velocities are shown to be proportional to the anisotropy level of the single crystals multiplied by the product of the two lowest eigenvalues of the local stiffness tensor. The former is inversely proportional to material's density.
Mots clés — random polycrystals, texture, phase velocity variation.

1 Introduction

Polycrystals comprise discrete grains exhibiting variable shapes, sizes, and crystallographic orientations, and thus, they reveal important fluctuations in their mechanical properties. The overall elastic modulus tensor of a polycrystal with infinite number of grains is a deterministic isotropic tensor. However, real polycrystals have a finite number of crystals which results in a non-zero anisotropy degree. Therefore, the overall mechanical properties of these polycrystals present variations between different samples. This has been observed in experimental works investigating the impact of the number of grains and medium size [1,3] as well as in numerical studies [4,8]. Sheng et al. [8] investigated the influence of the mean grain diameters and their dispersion level on the standard deviation of plane wave phase velocities propagating in textureless cubic equiaxed polycrystals. In this paper, we first derive analytical equations for the standard deviations of the effective elastic modulus tensor. We show the link between the latter and the microstructural parameters such as the mean and coefficient of variation of the grain diameters, the anisotropy level of single crystals, and the number of grains. Solving for the eigenvalues of Christofel's equation will further allow us to derive expressions for variabilities of the phase velocities. By introducing a parameter quantifying the texture level, and a universal anisotropy index, we show that the variance of the squared phase velocities is directly proportional to the product of the anisotropy level and the two lowest eigenvalues of the local elasticity tensor. The results obtained in this paper could be used for non-destructive microstructural characterization of polycrystals. Deviation from the analytical predictions could allow us to characterize regions exhibiting significantly distinct morphological or crystallographic properties, i.e., the presence of macrozones [2].

2 Theoretical framework

2.1 Statistics of effective medium properties

Let $\Omega \subset \mathbb{R}^3$ denote a randomly generated polycrystalline sample containing N_g equiaxed crystals, each of which occupied by a domain Ω_i with measure (volume) $V_i = (\pi/6)D_i^3$ where D_i is the equivalent diameter of i-th grain, $i \in [\![1, N_g]\!]$. To simplify the final results, we follow the classical lognormal distribution assumption for the equivalent diameter random variable D, i.e., $D \sim \text{lognormal}(\bar{D},\sigma_D)$. For this particular case, since *iid* random variables D_i follow a lognormal distribution, the volumes V_i are also lognormally distributed (with modified shape parameters). Each of these crystals has a different crystallographic

orientation that is characterized by triplets of Euler angles $(\Theta_1^{(i)}, \Theta^{(i)}, \Theta_2^{(i)})$. These are *iid* vectors of random variables distributed following the joint probability density function (PDF) defined as:

$$f_{(\Theta_1,\Theta,\Theta_2)}(\theta_1,\theta,\theta_2) = F(\theta_1,\theta,\theta_2)\frac{\sin(\theta)}{8\pi^2}1_{[0,2\pi]}(\theta_1)1_{[0,\pi]}(\theta)1_{[0,2\pi]}(\theta_2), \tag{1}$$

where $1_{\mathcal{D}}(x)$ specifies the indicator function (1 if $x \in \mathcal{D}$ and 0 otherwise) and the orientation distribution function (ODF) F writes:

$$F(\theta_1,\theta,\theta_2) = F_0 \exp\left(\frac{\cos(\theta_1)}{2\tau_{\theta_1}} + \frac{\cos(\theta)}{2\tau_{\theta}} + \frac{\cos(\theta_2)}{2\tau_{\theta_2}}\right), \tag{2}$$

where F_0 is a normalization factor such that $\int\int\int f_{(\Theta_1,\Theta,\Theta_2)}(\theta_1,\theta,\theta_2)\mathrm{d}\theta_1\mathrm{d}\theta\mathrm{d}\theta_2 = 1$ and can be obtained via $F_0 = (2\tau_\theta)^{-1}\mathrm{csch}((2\tau_\theta)^{-1})/[I(0,(2\tau_{\theta_1})^{-1})I(0,(2\tau_{\theta_2})^{-1})]$ where $I(\nu,z)$ is the modified Bessel function of the first kind of order ν. In equation (2), the ODF is modeled using a Gaussian-type distribution where the triplet $(\tau_{\theta_1},\tau_\theta,\tau_{\theta_2})$ represents three independent texture parameters that characterize the degrees of preferred orientation for crystallites along each respective direction. Two extreme cases of perfect clustering (resulting in a single orientation where the polycrystal degenerates to a single grain) and no clustering (uniformly distributed random orientations, corresponding to statistically isotropic polycrystals) can be obtained when the texture parameters tend to zero and infinity, respectively. Following Yang et al. [10], the texture parameters are modeled as $\tau_\theta = \tau$, $\tau_{\theta_1} = q_{\tau_{\theta_1}}\tau$ and $\tau_{\theta_2} = q_{\tau_{\theta_2}}\tau$ where τ is called the unified texture parameter and the factors $(q_{\tau_{\theta_1}}, q_{\tau_{\theta_2}})$ specify the relative degrees of texture in the corresponding directions. In this paper, for simplification purposes, we consider the particular case of one-parameter Gaussian ODF where $\tau_{\theta_1} = \tau_{\theta_2} \to \infty$ and $\tau_\theta = \tau$ describes the texture parameter (see Yang et al. [9]).

Figure 1 schematically depicts this aggregate of randomly packed grains. Since a statistical study of the homogenized elastic properties is to be carried out, the analytical averaging approaches based on Voigt, Reuss, and self-consistent are more appropriate thanks to their fast evaluation (see [4,8] for more details). We limit our focus to the Voigt average medium of equiaxed grains with cubic symmetry. The stiffness tensor is thus characterized with three elastic constants c_{11}, c_{12}, and c_{44}. The positive eigenvalues of the cubic stiffness matrix are $(\lambda_1,\lambda_2,\lambda_3) = (c_{11}+2c_{12}, 2c_{44}, c_{11}-c_{12})$. To quantify the anisotropy level of these cubic single crystals, we will use the universal anisotropy index $A^U \in \mathbb{R}^+$, introduced by Ranganathan and Ostoja-Starzewski [6], which is identically zero for isotropic crystals and increases for more anisotropic crystayls. For cubic crystals, $A^U = 6\nu_\mathrm{v}^2/(5\lambda_2\lambda_3)$, where $\nu_\mathrm{v} = c_{11} - c_{12} - 2c_{44}$ is called the anisotropy coefficient. The components of the Voigt average elastic modulus tensor read:

$$\mathbb{C}^{\mathrm{eff}}_{ijkl} = c_{12}\delta_{ij}\delta_{kl} + c_{44}(\delta_{ik}\delta_{jl}+\delta_{il}\delta_{jk}) + \nu_\mathrm{v}\frac{\sum_{m=1}^{N_g}\left(\sum_{n=1}^{3} A_{in}^{(m)}A_{jn}^{(m)}A_{kn}^{(m)}A_{ln}^{(m)}\right)V_m}{\sum_{m=1}^{N_g} V_m}, \tag{3}$$

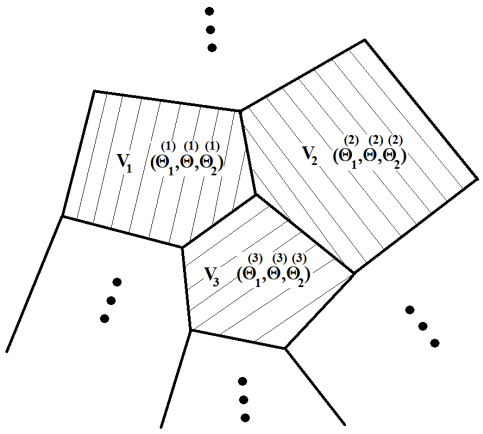

Figure 1: Schematic representation of a random polycrystal.

where δ_{mn} is the Kronecker delta (1 if $m=n$ and 0 otherwise), and $A(\theta_1,\theta(\tau),\theta_2)$ is the rotation matrix. The corresponding 6×6 matrix C_{IJ}^{eff} is further constructed via the following one-to-one mapping between a symmetric pair $(i,j)\in[\![1,3]\!]^2$ and a multi-index $I\in[\![1,6]\!]$: $11\leftrightarrow 1$, $22\leftrightarrow 2$, $33\leftrightarrow 3$, $23\leftrightarrow 4$, $13\leftrightarrow 5$, and $12\leftrightarrow 6$. Taking the standard deviation of both sides of Equation (3) yields the following general formula for the standard deviation of different components of the effective elastic modulus matrix, C_{IJ}^{eff}:

$$\sigma_{C_{IJ}^{\text{eff}}}=\frac{\alpha_{IJ}(\tau)|\nu_{\text{v}}|}{\sqrt{N_g}}\sqrt{\frac{\overline{D^{2d}}}{\overline{D^d}^2}}=\frac{\sqrt{5A^U\lambda_2\lambda_3}\alpha_{IJ}(\tau)(1+\delta_D^2)^{4.5}}{\sqrt{6N_g}}, \tag{4}$$

where $\delta_D=\sigma_D/\bar{D}$ and $\overline{D^n}$ denote the coefficient of variation and the nth moment of D, respectively. It is worth mentioning that $|\nu_{\text{v}}|$ includes the material-dependent part which implies that the variation of $\sigma_{C_{IJ}^{\text{eff}}}/|\nu_{\text{v}}|$ in terms of N_g results in a master curve. Note also that the last part of this equation is obtained for the particular case where D is distributed via a lognormal distribution. The components of interest of the matrix C_{IJ}^{eff} are $IJ=\{11,12,66\}$ for which the corresponding coefficients $\alpha_{IJ}(\tau)$ are reported in Sheng et al. [8] as $[\sqrt{16/525},\sqrt{9/525},\sqrt{9/525}]$, respectively. For a range of values for the texture parameter τ, these coefficients are numerically calculated and plotted in Figure 2(left and middle). These plots show larger variabilities for the components of C_{IJ}^{eff} when the texture parameter τ tends to zero. Convergence to non-preferential orientations occurs for $\tau>0.5$. As an example, sharp local textures associated with the clusters of α grains give rise to the so-called macrozones in some titanium alloys [2]. Higher variabilities of the effective properties of these samples are thus expected. Figure 2(right) depicts the change in the marginal distribution of the Euler angle θ between textureless case ($\tau\to\infty$, corresponding to the well-known Gilbert's sine distribution) and textured case where $\tau=0.07$. For this particular textured case, θ does not take any values in the interval $[\pi/2,\pi]$.

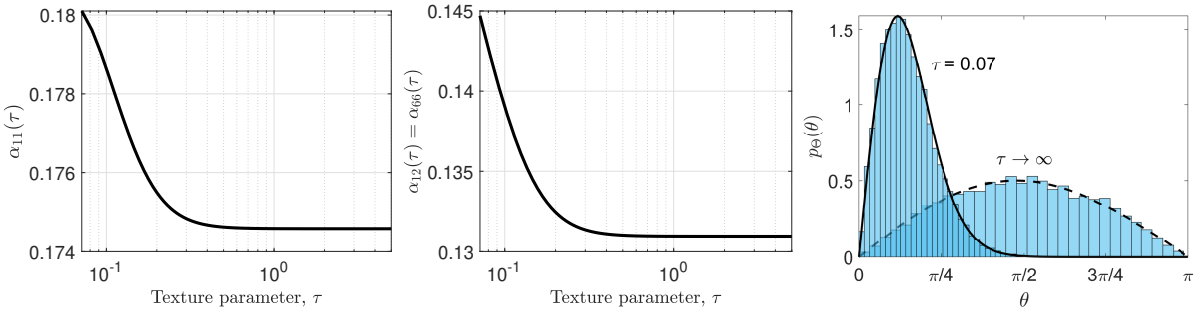

Figure 2: Coefficients α_{11} (left) and $\alpha_{12}=\alpha_{66}$ (middle) in terms of the texture parameter τ. PDFs of the Euler angle θ for textureless and textured polycrystals (right).

Note that the fluctuation level of C_{11}^{eff} is always larger than that of C_{12}^{eff} and C_{66}^{eff}, regardless of the value of the texture parameter τ. It is worth mentioning that changing the homogenization method will change the term $|\nu_{\text{v}}|$ in Equation (3) (see [4,8] for more details). In Sheng et al. [7], a random field-based modeling of Euler angles is used to take into account the texture, where the correlation lengths are employed instead of the texture parameters $(\tau_{\theta_1},\tau_\theta,\tau_{\theta_2})$.

2.2 Statistics of phase velocities

The phase velocities v_i (i specifies the mode type: compression P, fast shear S_1 and slow shear S_2) and their corresponding polarization directions $\mathbf{w}_i$ can now be determined by solving the Christoffel equation $(\mathbb{C}_{mnop}^{\text{eff}}\hat{k}_n\hat{k}_o-\rho v^2\delta_{mp})w_p=0$ where $\hat{\mathbf{k}}$ is the propagation direction, and ρ is the density of the material considered deterministic constant. Since the background elastic modulus tensor is not deterministic, the eigenvalues and eigenvectors of the symmetric second-order tensor $\Lambda_{mp}=\mathbb{C}_{mnop}^{\text{eff}}\hat{k}_n\hat{k}_o$ are also random variables. Let a plane wave propagate following $\hat{\mathbf{k}}=[1\ 0\ 0]^\top$, the phase velocities of the modes $i\in\{\text{P},\text{S}_1,\text{S}_2\}$ are then determined by $\rho v_i^2=C_{IJ}^{\text{eff}}$ where $IJ\in\{11,66,55\}$, respectively. As a result, the standard deviations of the squared phase velocities are directly linked to those of the components of the

effective elastic modulus tensor of the medium:

$$\sigma_{v_i^2} = \frac{\alpha_{IJ}(\tau)|\nu_v|}{\rho\sqrt{N_g}}\sqrt{\frac{\overline{D^{2d}}}{\overline{D^d}^2}} = \frac{\zeta\alpha_{IJ}(\tau)\left(1+\delta_D^2\right)^{4.5}}{\sqrt{N_g}}, \tag{5}$$

wherein $\zeta = |\nu_v|/\rho = \sqrt{(5/6)A^U\lambda_2\lambda_3}/\rho$. A normalization of the standard deviation by ζ, i.e. $\sigma_{v_i^2}/\zeta$, yields a master curve, regardless of the material properties. Even though $\sigma_{v_i^2}$ is proportional to the square root of the universal anisotropy level, the latter cannot solely determine which material has more or less variability in squared phase velocity. Instead, larger (resp. smaller) values of ζ imply larger (resp. smaller) variability in squared phase velocities.

In practice, when ultrasonic measurements are conducted over a sample of volume $|\Omega| = V_s$, one approach to analytically predict the variability of squared phase velocities is by approximating the number of grains N_g via $V_s/((\pi/6)\bar{D}^3(1+\delta_D^2)^3)$. This yields the following estimator:

$$\sigma_{v_i^2} = \frac{\sqrt{\frac{\pi}{6}}\zeta\alpha_{IJ}(\tau)\bar{D}^{1.5}\left(1+\delta_D^2\right)^6}{\sqrt{V_s}}. \tag{6}$$

3 Numerical results

In this section, we aim to validate the analytical results in Section 2 via numerical simulations. For this purpose, we generate polycrystalline samples using the open-source software Neper [5]. An example of these samples along with the PDF of the grain equivalent diameters are depicted in Figure 3. The number of grains are $N_g = D\times 10^E$ with $D\in\{1,5\}$ and $E\in[\![2,6]\!]$, and for each value of N_g, 200 realizations are generated by reshuffling the seeds used to generate the grains and by re-randomizing the crystallographic orientations. The latter are generated for large values of the texture parameter τ (textureless). Moreover, three different values for the dispersion level of the grain equivalent diameters are considered, $\delta_D\in\{0.25,0.5,0.75\}$. Following [8], five cubic materials are considered with increasing anisotropy levels (from aluminium to lithium). The elastic constants, densities, universal anisotropy indices A^U and the values of the parameter ζ are summarized in Table 1.

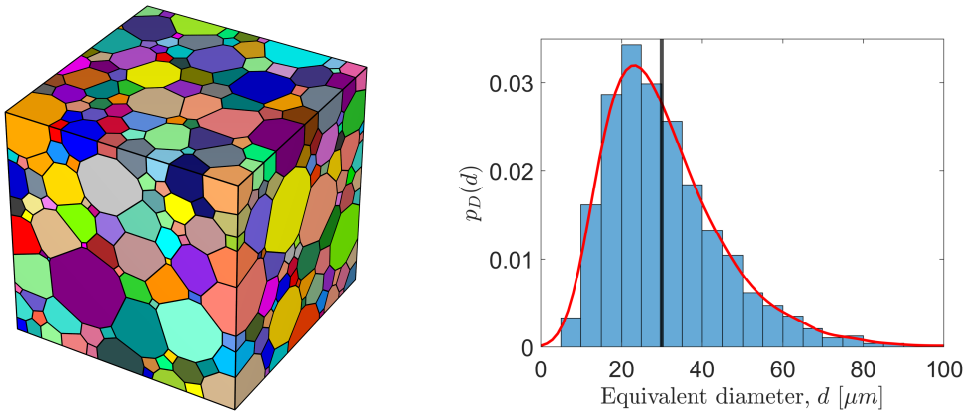

Figure 3: A realization of a polycrystalline aggregate with 10^3 grains (left) whose equivalent diameters follow a lognormal distribution with the following parameters $\bar{D} = 30$ μm, and $\delta_D = 0.25$ (right).

Figure 4(left) shows the variation of the standard deviation of squared P-wave velocity in terms of the number of grains for different values of δ_D. In this figure, black solid lines are those obtained using the analytical formula (5). From bottom to top, the lines correspond to $\delta_D = 0.25$, 0.5, and 0.75, respectively. The blue markers are the results obtained based on synthetic samples by considering a plane wave propagating in $\hat{\mathbf{k}} = [1\ 0\ 0]^\top$ direction. As for the red markers, we also did a statistical averaging over the entire direction space, generated uniformly over a unit sphere. The results from both types of simulations are in general in good agreement with the analytical predictions. However, a discrepancy is observed for large values of δ_D and small number of grains ($N_g < 5\times 10^3$). The reason is that, for these cases, 200 realizations are not statistically sufficient to accurately represent the microstructure of

Table 1: Elastic constants and densities of different cubic materials considered in this study (taken from [8]).

Name	c_{11} [GPa]	c_{12} [GPa]	c_{44} [GPa]	ρ [kg/m^3]	A^U [$-$]	$\zeta \times 10^7$ [(m/s)^2]
Al	108	62	28.3	2700	0.05	0.43
α-Fe	231	135	115	7860	0.98	1.88
Co	242	160	128	8900	1.73	2.14
γ-Fe	154	122	77	8000	3.62	1.67
Li	13.4	11.3	9.6	534	8.70	3.51

the polycrystal. Therefore, by using a larger number of samples, the blue and red markers will converge toward the analytical solid lines. Note that similar results are obtained for the standard deviations of fast and slow shear wave velocities, although they are not presented here for the sake of brevity.

In Figure 4(right), we compared the variation of $\sigma_{v_p^2}$ in terms of N_g for different cubic materials listed in Table 1. It can be observed that, increasing in the values of $\sigma_{v_p^2}$ does not necessarily occur by increasing the anisotropy level A^U. In contrast, the values of the parameter ζ (last column of Table 1) determines the level of variability in the squared phase velocities.

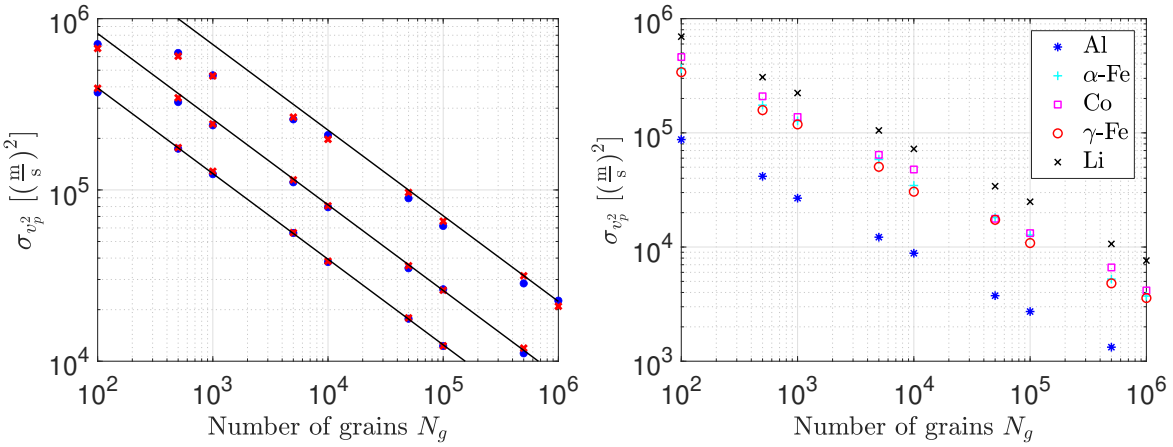

Figure 4: Standard deviation of squared P-wave velocity for three different values of δ_D. Solid black lines indicate the analytical predictions (δ_D increases from bottom to top). Blue and red markers correspond to the results obtained using synthetic polycrystals (left). The standard deviation of squared P-wave velocity for five cubic materials with different anisotropy levels (right).

4 Conlusions

In this paper, the analytical framework developed by Sheng et al. [8] is extended to the case of textured random polycrystals. Instead of a random field-based approach to model the crystallographic orientations introduced in Sheng et al. [7], we used a model for the orientation distribution function. The variation in the squared phase velocities could be estimated based on elastic parameters, morphological characteristics (mean and standard deviation of equivalent grain diameters) and a unified texture parameter. Extending these results to the case of materials with hexagonal symmetry will be carried out in a future work.

References

[1] F. Chen, S. Chen, X. Dong, C. Li, X. Hong, X. Zhang. *Size effects on tensile strength of aluminum–bronze alloy at room temperature*, Materials & Design. 85, 778–784, 2015.

[2] L. Germain, N. Gey, M. Humbert, P. Bocher, M. Jahazi. *Analysis of sharp microtexture heterogeneities in a bimodal IMI 834 billet*, Acta Materialia, 53(13), 3535-3543, 2005.

[3] J. Kim, R. Golle, H. Hoffmann. *Investigation of size effects of very thin aluminum and copper sheets using aero-bulge test*, Materials Science and Engineering: A, 527(27-28), 7220-7224, 2010.

[4] M. Norouzian, J.A. Turner. *Ultrasonic wave propagation predictions for polycrystalline materials using three-dimensional synthetic microstructures: Phase velocity variations*, The Journal of the Acoustical Society of America, 145, 2171–2180, 2019.

[5] R. Quey, P.R. Dawson, F. Barbe. *Large-scale 3D random polycrystals for the finite element method: Generation, meshing and remeshing*, Computer Methods in Applied Mechanics and Engineering, 200(17-20), 1729-1745, 2011.

[6] S. I. Ranganathan, M. Ostoja-Starzewski. *Universal elastic anisotropy index*, Physical review letters, 101(5), 055504, 2008.

[7] N. Sheng, S. Khazaie, M. Chevreuil, S. Fréour. *Statistical properties of effective elastic moduli of random cubic polycrystals*, Mechanics Industry, 24, 33, 2023.

[8] N. Sheng, S. Khazaie, M. Chevreuil, S. Fréour. *On the statistical behavior of homogenized properties and ultrasonic phase velocities in random polycrystals*, International Journal of Solids and Structures, 285, 112531, 2023.

[9] L. Yang, O. I. Lobkis, S.I. Rokhlin. *Ultrasonic propagation and scattering in duplex microstructures with application to titanium alloys*, Journal of Nondestructive Evaluation, 31, 270-283, 2012.

[10] L. Yang, S. I. Rokhlin. *Ultrasonic backscattering in cubic polycrystals with ellipsoidal grains and texture*, Journal of Nondestructive Evaluation, 32, 142-155, 2013.